

\$

A machine vision system for quality grading of painted slates

By

Ovidiu Ghita, Tim Carew and Paul F. Whelan

The major aim of this chapter is to detail the technology associated with a novel industrial inspection system that is able to robustly identify the visual defects present on the surface of painted slates. The development of a real-time automated slate inspection system proved to be a challenging task since the surface of the slate is painted with glossy dark colours, the slate is characterised by depth profile non-uniformities and it is transported at the inspection line via high-speed conveyors. In order to implement an industrial compliant system, in our design we had to devise a large number of novel solutions including the development of a full customised illumination set-up and the development of flexible image-processing procedures that can accommodate the large spectrum of visual defects that can be present on the slate surface and the vibrations generated by the slate transport system. The developed machine vision system has been subjected to a thorough robustness evaluation and the reported experimental results indicate that the proposed solution can be used to replace the manual procedure that is currently used to grade the painted slates in manufacturing environments.

\$.1 Introduction

Over the past three decades the deployment of vision-based solutions in the development of automatic inspection systems has witnessed a substantial growth. This growth was motivated in part by the increased flexibility attained by the vision-based industrial inspection solutions when applied to the classification of the manufactured products with respect to their aesthetical and functional characteristics and equally important these

systems opened the opportunity to control the production process by evaluating the statistics that describe the efficiency of the overall manufacturing process. In this context it is useful to mention that slate manufacturing is a highly automated process where product inspection being the solely task that is still performed by human operators. In this process, the human operators analyse the slates visually when they emerge via a conveyor from the paint process line and they make a judgement whether the produced units have a surface finish of acceptable quality or not. If defective slates are detected during visual inspection, they are removed from the production line and put aside for rework or rejection. Although the in-line manual inspection generates accurate results when applied to product quality assessment, it is highly reliant on the pictorial information perceived by the human visual system (HVS) [1-3] and as a consequence it is critically influenced by the experience and the acuity of the human operator. In addition to this, it is important to note that the performance of the human operator is not constant and moreover the manual inspection represents a monotonous work that cannot be used in conjunction with high-speed product manufacturing lines. In this context, Tobias et al [3] list some of the key factors that justify the adoption of machine vision systems in industry. These are increased productivity, improved product quality, absence of human inspectors performing dull and monotonous tasks, high-speed inspection (matched by high-speed production) and reduced human labour costs. In particular we would like to stress that the incorporation of automation in manufacturing industry is not necessarily about the displacement of labour, but more as an answer to the expectation of an increasingly educated labour force and the compliance to the recent realities of the world economy [4].

However, the design of industry compliant machine vision systems is far from a trivial task as several issues including the mechanical design, development of an appropriate illumination set-up, optimal interfacing between the sensing and optical equipment with the computer vision component have to be properly addressed in order to accommodate all challenges that are encountered in a typical industrial environment [5-7,27]. In this regard, the aim of this chapter is to detail the development of fully integrated machine vision system that has been specifically designed to assess the surface quality of the painted slates. In this chapter we will discuss in detail the design choices that were made in the development phase of the proposed vision sensor and we will also describe the algorithmic solutions that were implemented to accommodate the large variation of the structural and paint defects that are present on the surface of the painted slates. This chapter is organised as follows. Section 2.2 discusses the related systems that have been documented in the literature. Section 2.3 provides a description of the typical slate defects and the discussion is continued in Section 2.4 with the brief presentation of the developed slate inspection system. In Section 2.5 the adopted illumination set-up is detailed. Section 2.6 details the image processing

inspection algorithm, while in Section 7 the challenges introduced by factory conditions are analysed. Section 8 presents the experimental results, while Section 9 concludes this chapter.

2 Related vision-based inspection systems

Although the application of machine vision solutions in the development of industrial systems is a well-documented topic of research, we were not able to identify any relevant work on the inspection of painted slates. However, following a detailed search on the specialised literature we were able to find a large number of approaches that have been proposed to address the automatic inspection of ceramic tiles [3,8-11,13,23,24], which are products that have several common characteristics with painted slates. Thus, although the manufacturing processes for slates and ceramic tiles are different, both products have rectangular shapes, have textured surfaces and they are transported at the inspection point via conveying means [2]. Also, the defects associated with ceramic products resemble characteristics that are common with the visual defects that are specific for painted slates, but the range of defects (types and sizes) for ceramic products is substantially reduced when compared to the large variety of slate defects.

The works in the field of ceramic tile inspection reviewed in this chapter employed a large spectrum of different imaging sub-systems and processing techniques to detect the visual defects that may be present on the surface of the product. One issue that has to be accommodated during the development phase of the developed inspection systems was the relative large range of structural and paint defects that can be encountered during the manufacturing process. In order to address this challenging scenario, the advantages associated with the multi-component inspection process start to become apparent. In this regard, the vast majority of reviewed systems approached the inspection process in a modular fashion where each component has been customised to identify a specific category of defects. To further improve the performance of the defect identification module, a critical issue was the adoption of appropriate opto-mechanical and sensorial equipment and the optimisation of the illumination set-up. Thus, most ceramic inspection systems employed line scan cameras to minimise the spatial non-uniformities during the image acquisition process and this option was also motivated by the fact that conveying means were invariable used to transport the products to the inspection line. (The use of standard array CCD/CMOS cameras was rarely noticed and this imaging solution has been primarily employed in the development of prototype systems.) The use of line scan cameras has alleviated to some extent the requirement to devise complex illumination arrangements, as the light intensity has to be maintained uniform only along a narrow stripe area (that is imaged by the line-scan sensors). To

this end, the ceramic inspection systems examined in our review employed either diffuse [8-12] or collimated lighting set-ups [1,2,11-12].

In line with the optimisation of the opto-mechanical components, the development of robust image-processing procedures to detect the visual defects proved to be a key element to the success of the overall inspection system. Our survey on ceramic tile inspection revealed that two approaches were dominant, namely approaches that perform the identification of the visual defects using either morphological techniques [1,12-17] or inspection solutions based on texture analysis [2,18-23]. From these approaches, the morphological-based implementations proved prevalent as they offer efficient implementations that are capable of real-time operation. In this regard, Boukouvalas et al [9] employed 1D convolvers in the horizontal and vertical directions to identify the line and spot defects on the surface of the coloured ceramic tiles. In their implementation, the filter coefficients are tuned to capture a narrow range of line widths and this fact substantially complicates the generalisation of this approach if it will be re-engineered to encompass the wide variety of visual defects present on the surface of the slates. This work was further developed by the authors in [10,11] where they developed more involved techniques that have been applied to inspect the coloured and patterned ceramic tiles. In [10] the authors introduced a clustering approach that has been applied to segment the image data captured from a patterned tile into background and foreground information. In this study, the authors were particularly concerned with the development of a simple correction procedure that aimed to alleviate the spatial and temporal non-constancies that were inserted by the imperfections in the illumination set-up and non-linearity response of the imaging sensor. Although the authors did not provide numerical results to quantify the accuracy of the proposed approach, this paper is a good example that illustrates the range of problems that need to be addressed in the implementation of machine vision systems. A different approach was proposed in [9] where the authors discussed the application of Wigner distributions to the inspection of patterned tiles. Although this approach is interesting as it can be applied to the inspection of a large palette of ceramic products, it has less relevance to slate inspection as the surface of the painted slates is characterised by a mild non-regularized texture. Peñaranda et al [8] proposed an alternative approach that has potential to be applied to slate inspection. In their paper, the authors proposed an inspection algorithm that evaluates the local gray-scale intensity histograms as the main discriminative feature in the process of identifying the defective image regions. Unfortunately, when we applied this solution to slate inspection, this approach proved unreliable since we found out that the grayscale distributions vary considerable from slate to slate when they emerge from the paint line. In addition to the inter-slate grayscale intensity variation, the low statistical impact of the small defects on the profile of the intensity distributions precludes the use of *a priori* patterns that are able to

encompass the variations within image regions of acceptable finish quality. A related approach was proposed by Boukouvalas et al [11] where colour histograms have been employed to sample chromato-structural properties of patterned ceramic tiles. In this work the authors attempted to address a large range of issues including the evaluation of robust similarity metrics, spatial and temporal colour normalisation and the development of a computationally efficient hierarchical colour representation scheme. A few years later, this approach was further developed by Kukkonen et al [23] where they extracted 10 local features from the local distributions calculated in the hyper-spectral domain. The main motivation to use hyper-spectral data resides in the fact that it samples in a more elaborate manner the spectral properties of the ceramic tiles than the standard RGB data [25], but the experimental results reveal that the best performance was achieved when normalised *rgb* chromaticity values were used for classification purposes.

As mentioned earlier, a distinct area of research was concerned with the application of texture-based approaches in the development of product inspection systems. Approaches that are included in this category include the work of Tobias et al [3], Ojala et al [26], Mäenpää et al [18] and Mandriota et al [22]. These methods addressed a large range of industrial inspection applications and the most promising technique when evaluated in conjunction to the inspection of painted slates was the *local binary pattern* (LBP) approach that was initially developed by Ojala et al [26]. To this end, in a recent publication [2] we have developed an automatic slate inspection system where the texture and tonal (grayscale) information were adaptively combined in a split and merge strategy. The experimental results proved the effectiveness of this approach (99.14 per cent), but the main limitation was the large computational time required to process the slate image data.

From this short literature survey we can conclude that the development of a robust algorithm for slate inspection is a challenging task since a large number of issues relating to the opto-mechanical design and the selection of appropriate image processing procedures have to be addressed. During the development phase of the proposed prototype we were forced to adopt a modular approach as the slate's grayscale information shows a heterogeneous distribution with substantial inter-slate intensity variations. Moreover, in our design we had to confront other challenging issues including the depth profile variations (slate bowing) and vibrations that were introduced by the slate transport system.

\$.3 Description of the visual defects present on the surface of painted slates

The slates are manufactured using a mix of raw materials including cement, mineral and synthetic fibres and after they are structurally formed

and dried, they are automatically painted on a high-speed line. While the primary function of the slates is to prevent water ingress to the building, they also have certain aesthetic functions. Consequently, the identification of visual defects is an important aspect of the slate manufacturing process and to answer this requirement inspection procedures are in place to ensure that no defective products are delivered to customers. Currently, the slates are manually inspected by human operators and they make a decision as to whether each individual product is defect free and remove the slates that are not compliant to stringent quality criteria. To this end, the products meeting the quality criteria need to be correctly formed (having an undistorted rectangular shape with minor deviations from a planar surface) and their top surface should be uniformly painted in dark grey with a high gloss finish (the characteristics of the manufactured slates are listed in Table 1).

Dimension	Nominal	Tolerance
Length	600 mm	±3 mm
Width	300 mm	±3 mm
Thickness	4.0 mm	±0.1 mm
Local flatness profile	±0.1 mm	±0.1 mm
Concavity	±0.05 mm	±5 mm
Convexity	±0.05 mm	±5 mm

Table 1. The main characteristics of the manufactured slates.

An interesting aspects associated with the manual slate inspection is to evaluate the frequency of the minor and repetitive faults that may occur when the slates are painted. This information can be used to correct the improper settings of the high-speed paint line and to allow the efficient sorting of the finite products into batches with uniform characteristics.

As the slate manufacturing process entails two major production stages, namely the slate formation and slate painting, the visual defects can be divided into two broad categories: substrate and paint defects. Thus, substrate defects include incomplete slate formation, lumps, depressions and template marks, whereas paint defects include no paint, insufficient paint, paint droplets, orange peel, efflorescence and paint debris. The substrate and paint defects may have arbitrary shapes and their sizes range from 1 mm² to hundreds of square mm. Table 2 details a comprehensive list of most common visual defects present on the surface of defective slates, where for each defect type a brief description is provided.

No.	Defect type	Defect size	Description
1	Lumps	$2.0 \text{ mm} < \{L, W\} < 50 \text{ mm}$ $\pm 0.1 < H < \pm 3.5 \text{ mm}$	Excess material on surface. Often conical shape.
2	Depressions	$2.0 \text{ mm} < \{L, W\} < 50 \text{ mm}$ $\pm 0.1 < D < \pm 3.5 \text{ mm}$	Insufficient material on surface. Often inverse conical shape.
3	Holes	$\phi = 4.5 \text{ mm}$	Holes are present to assist insertion of nails. Absence indicates fault.
4	Incomplete slate	Any $W \neq W_{\text{expected}} \pm 3.0 \text{ mm}$ Any $L \neq L_{\text{expected}} \pm 3.0 \text{ mm}$	W, L dimensions not conforming to production specification.
5	Poor quality edge	$W = 0.2 \text{ mm} * L > 10 \text{ mm}$	Edge not straight or having a feathery feel.
6	Template mark	$0.5 < \{L, W\} < 600 \text{ mm}$ $0.1 < \{D, H\} < 3.0 \text{ mm}$.	Excess material on the slate surface caused by damage to forming template.
7	Template mark II	$1.0 \text{ mm} < d < \text{all slate}$	Texture variation on the slate surface, usually roughness.
8	Insufficient paint	$20 \text{ mm} < \{W, L\} < \text{all slate}$	Shade variation due to insufficient paint usage.
9	Missing paint	$2 \text{ mm} < \{W, L\} < \text{all slate}$	No paint or incomplete painting.
10	Droplet	$2 \text{ mm} < \{W, L\} < 15 \text{ mm}$ $0.05 \text{ mm} < D < 0.5 \text{ mm}$	Excess paint on surface, dried and cracked.
11	Efflorescence	Area $> 25 \text{ mm}^2$	Contaminant on surface preventing the correct adherence of paint.
12	Paint debris	$2 \text{ mm} < \{W, L\} < 50 \text{ mm}$	Dried paint debris encrusted on slate surface giving a rough texture.
13	Orange peel	$20 \text{ mm} < \{W, L\} < \text{all slate}$	Shade variation caused by overheating the slate.
14	Barring	$W = 10 \pm 5 \text{ mm}$ $20 < L < 600 \text{ mm}$	Shade variation caused by uneven heating of slate.
15	Spots	$1 \text{ mm} < \{W, L, \phi\} < 5 \text{ mm}$	Small areas presenting shade variation.
16	Nozzle drip	$W = 10 \pm 5 \text{ mm}$ $20 \text{ mm} < L < 600 \text{ mm}$	Shade variation caused by uneven paint delivery from nozzle.
17	Wax mark	$5 \text{ mm} < \{W, L\} < 50 \text{ mm}$	Splash of wax on top surface.

Table 2. A brief description of the visual defects. (Notations: L- length, W – width, ϕ - diameter, D – depth, H - height).

To further aid the reader in the process of interpreting the variability of the visual defects that may occur during the slate manufacturing process, a number of representative paint and substrate defects are depicted in Figures \$.1 and \$.2, where Figure \$.1(a) illustrate a defect-free slate image section.

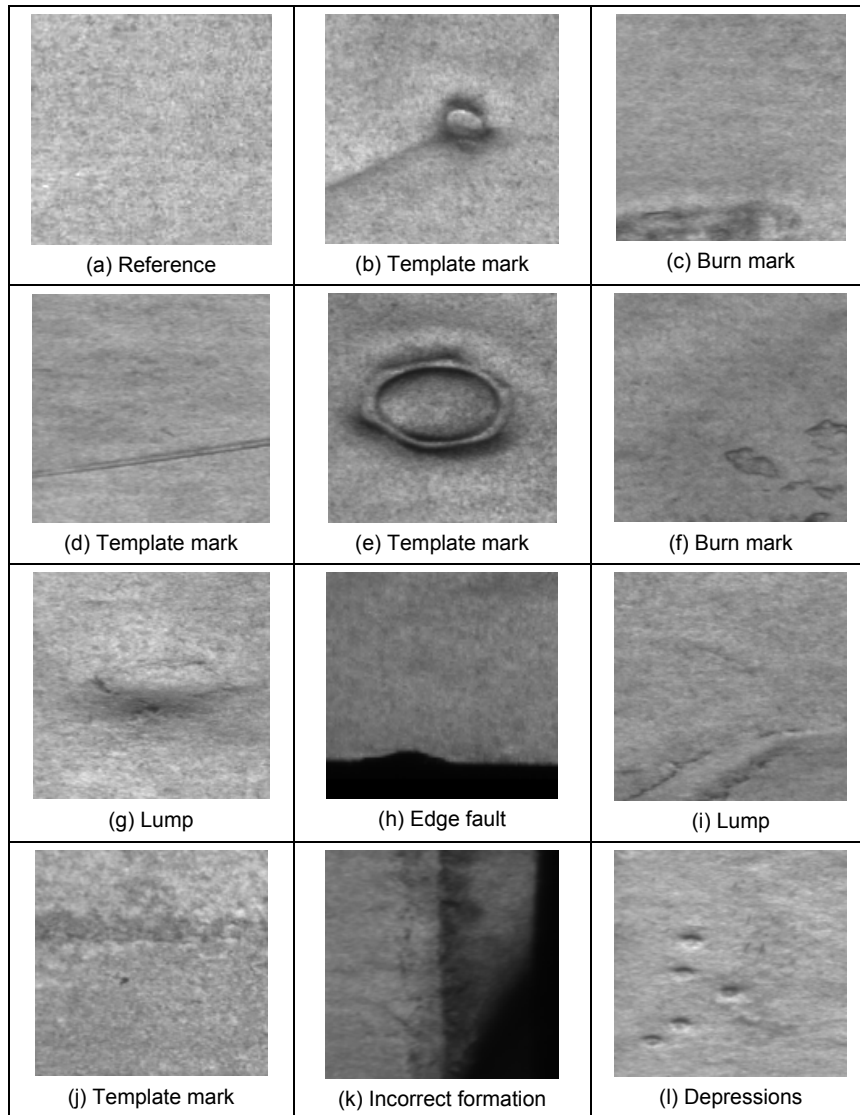


Figure \$.1. A selection of representative substrate defects including template mark, lump, depressions, burn mark and incorrect slate formation. (a) Defect-free slate section. (b-l) Defective slate section.

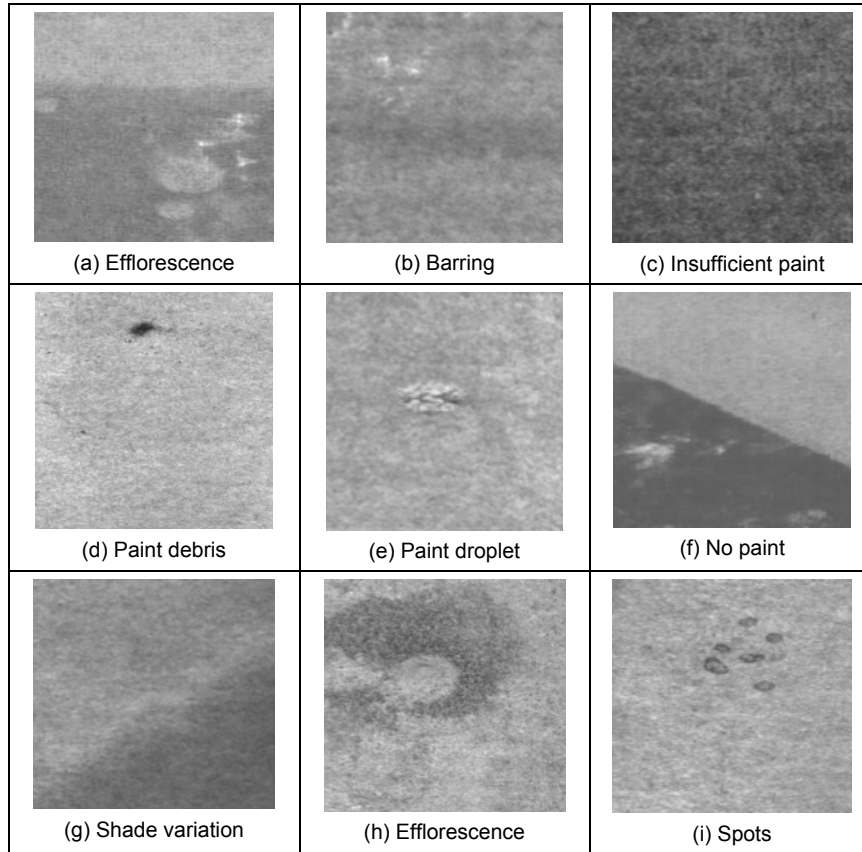


Figure \$.2. A selection of representative paint defects including efflorescence, no paint, insufficient paint, paint droplet, shade variation, paint debris, barring and spots.

\$.4 Overview of the developed slate inspection system

In order to devise a flexible machine vision solution, we have adopted a modular approach in our design. The prototype slate inspection system was built to closely replicate the manufacturing environment and consists of three main modules. The flowchart detailing the logical connections between constituent modules is illustrated in Figure \$.3. All modules of the developed inspection systems are controlled by an industrial PC which is also the host of the image processing software that has been designed to perform the classification of the slates into acceptable and defective products.

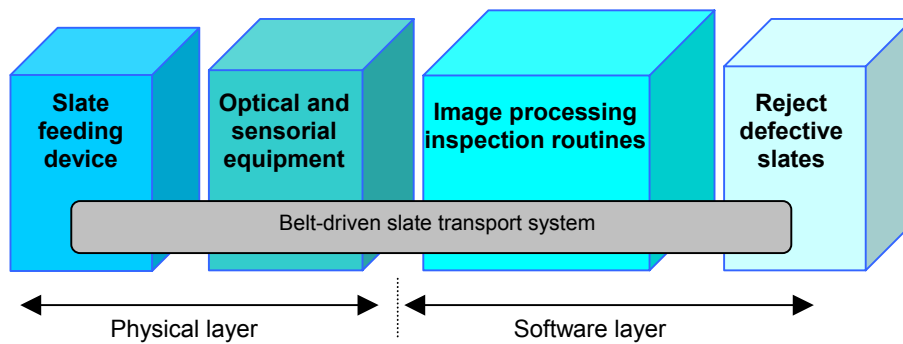


Figure \$.3. Overview of the designed slate inspection system.

The first module consists of the part feeding and the mechanical interface (slate transport system). In our implementation we have employed a two-metre long belt-driven industrial conveyor manufactured by Noretsyde Conveyors and Elevators (Ireland) that has been constructed to minimise the vibrations during the slate transport. An important issue was the selection of the belt material that minimises the amount of reflective light arriving back of the camera. After a careful selection, we have chosen a belt that is coated with a matte black rubber material that has low specular properties. To minimise the lateral drifts and slate rotations, a guide was placed on one side of the conveyor.

The second module of the slate inspection system is represented by the optical and sensing equipment. In the development of our slate inspection sensor we have used a Basler L102 2K-pixel line-scan camera which is fitted with a 28 mm standard machine vision lens (aperture set to 2.8). The line-scan camera operates at a scan frequency of 2.5 KHz. To allow a facile calibration of the sensing equipment with the illumination unit, the line-scan camera was attached to a micropositioner that allows fine adjustments to the camera view line with respect to the xyz coordinates. The camera set-up is illustrated in Figure \$.4. The interface between the camera and the industrial PC computer was facilitated by a Euresys frame grabber. Another important component of the optical and sensing module is represented by the illumination set-up. In our implementation we have design a collimated light arrangement that relies on the strong reflective properties of the slate's surface (full details about the implementation of the illumination set-up used in our design will be provided in the next section of this chapter). The last component of this module is represented by a proximity sensor which has the role to trigger the image acquisition process prior to the arrival of the slate at the inspection line.

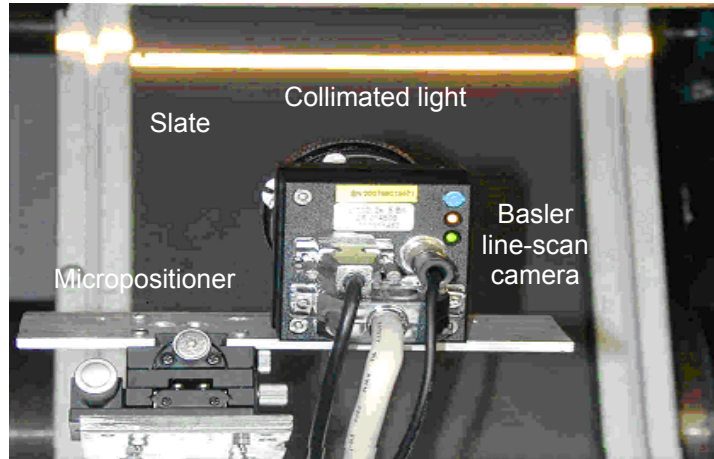


Figure \$.4. The Basler-2K line scan camera mounted on a xyz micropositioner that facilitates fine adjustments of the camera line view.

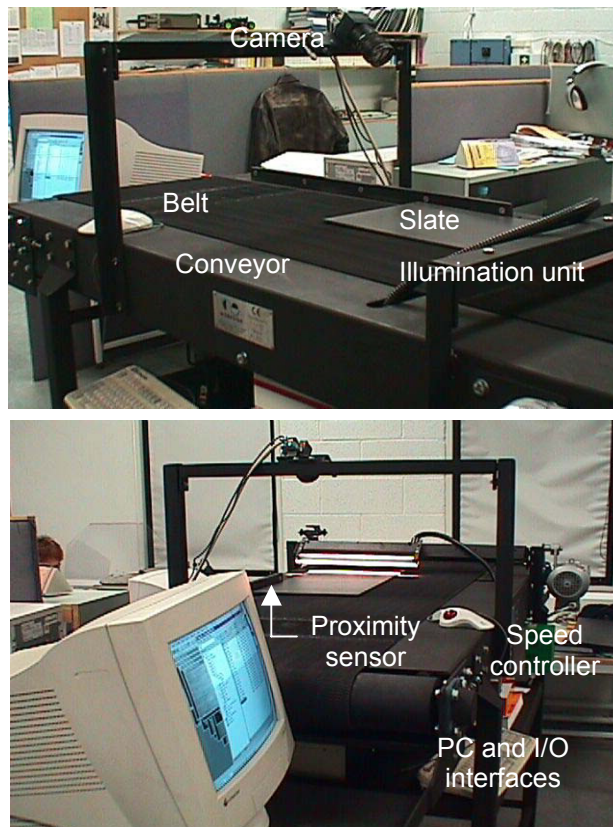


Figure \$.5. The prototype slate inspection system [1].

The final module of the system performs the identification of the visual defects in the image data captured by the line-scan camera. While the development of a single procedure to identify all types of defects detailed in Table 2 was not feasible, the proposed inspection algorithm has been also designed in a modular fashion where each component has been tailored to identify one specific category of defects (the proposed inspection algorithm will be detailed in Section 5.6). The developed prototype slate inspection system is illustrated in Figure 5.5.

5.5 Illumination set-up

The strategy used to image the slate relies on the strong reflecting properties of the slate surface. In our experiments we have tested several illumination set-ups involving diffuse and collimated lighting arrangements. Initially, diffuse lighting techniques were explored as this illumination technique generates a uniform wide light band that will offer a facile camera calibration. Thus, the first experiments were carried out using an aperture fluorescent light system with a cylindrical focusing lens (TSI Model AFL9000), where light is dispersed equally in a 60° arc. One important aspect when designing our set-up was the identification of the lamp angle of incidence that generates the strongest optical signal that is reflected back to the line-scan camera. In our experimental trials we have discovered that the optimal optical response was achieved when the lamp angle of incidence was set at 40° and the camera was symmetrically located at 40° relative to the slate position. With this arrangement the camera exposure time was set to 2ms and at this setting the moving direction pixel resolution was approx. 2 mm when the conveyor was operated at production line speeds. This resolution is not sufficient to identify the small and medium sized visual defects and our additional tests confirmed that the light intensity produced by diffuse lighting techniques is substantially lower than that required to properly image the slates at the inspection line speed. Consequently, our efforts were concentrated on the development of an alternative illumination set-up that involves a customized collimated lighting approach.

The collimated illumination solution adopted in our implementation is building on the fact that the paint defects have reduced gloss levels (except paint droplets) than the slate areas of acceptable quality. Substrate defects are associated with errors in slate formation and the resulting appearance of these visual defects also results in a reduction of the light arriving at the line-scan sensing element. The illumination arrangement comprises two Fostec DCR III 150W lamp controllers, a Fostec 30" fiber optic light line and a cylindrical lens. A schematic description of the devised illumination set-up is illustrated in Figure 5.6. The lamp angle of incidence has been set to 45° and the camera view angle was located symmetrically to 45°. The lamp intensity level was set to

approx. 80% with respect to the maximum level and the camera exposure time was set to 400 μ s at a scan frequency of 2.5 KHz. This setting allows us to image the slate with a cross pixel resolution of 0.221 mm and a moving pixel resolution of 0.244 mm. This pixel resolution is sufficient to properly image the entire range of defects that are present on the surface of the painted slates.

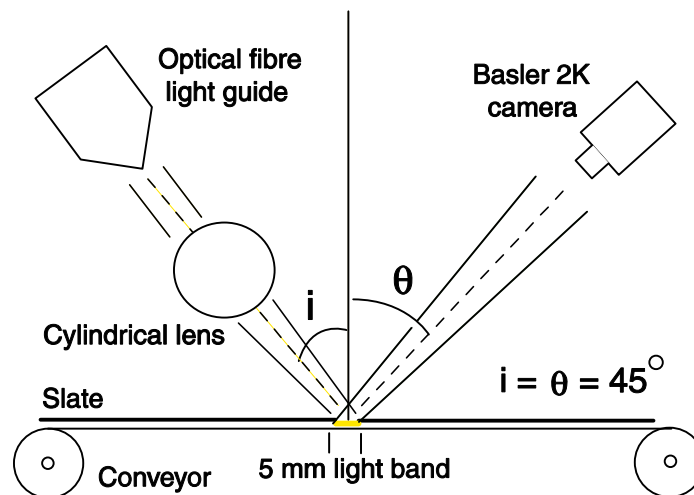
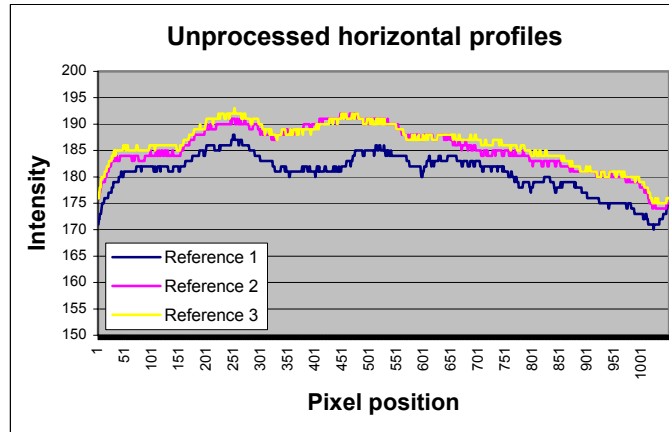


Figure \$.6. Schematic detailing the developed illumination set-up.

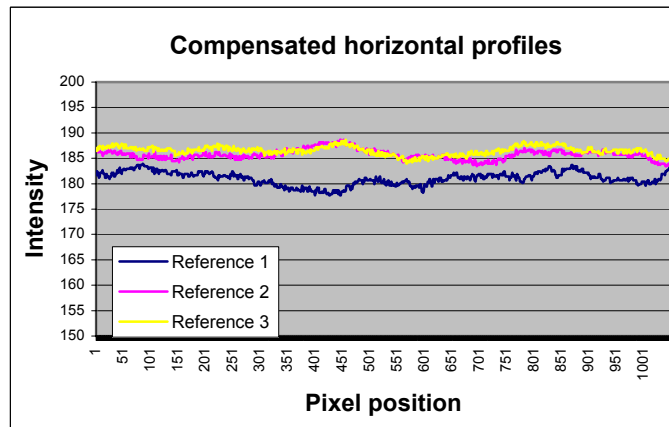
Although the illumination set-up detailed in Figure \$.6 generates sufficient illumination levels required for image acquisition at production line speeds, one issue that we encountered was the narrow band of the focused collimated light. Indeed, when we positioned the lens to attain perfectly focused collimated light, the resulting light band was only 5 mm wide (see Figure \$.6) and the process required to align the camera line view for a distance of 30" requires adjustments with a precision of less than one degree ($\delta\theta < 1^\circ$). To facilitate such adjustments we mounted the camera on a micropositioner as indicated in Section \$.4. However, the alignment of the camera line view to the longitudinal axis of the light band was not the only issue we had to confront during the development phase of the illumination set-up. One of the most challenging problems was the variation in depth profiles across the slate due to slate bowing that is sometimes associated with slates that have acceptable quality with respect to inspection criteria. The small slate bowing was found to range from negligible to 5 mm over the slate length and up to 2 mm along the slate width. Although the variation in depth profile does not affect the functionality of the product, it has introduced a substantial challenge that has to be accommodated by the proposed illumination solution. While the depth profile non-uniformities raises and lowers the absolute position of

the projected light band with respect to the camera line view, this practically compromises the image acquisition process. To give some insight into the problem generated by slate bowing, if we consider that the incidence of the light band and the camera view angle are set symmetrically to 45° as illustrated in Figure 6, if the slate raises the light band with 1 mm, then the reflected light is shifted to 1.5 mm in opposite direction with respect to the camera view line. Since the slate possesses some elasticity, a pneumatic solution that forces the slate into an uniformly planar shape during inspection would be feasible. However, there are several disadvantages associated with such mechanical solutions that are used to force the slate into the nominally flat shape. The first is related to fact that the painted surface can be easily damaged when the pneumatic device is operated at high production line speeds, and secondly the development of such mechanical system would be problematic taken into consideration the non-smooth characteristics of the underside of the slate. As a mechanical solution to force the slate into a uniform flat position proved unfeasible, we elected to defocus the lens that is used to collimate the light generated by the Fostec fiber optic light line. This produces a wider light band but this is achieved at the expense of reduced collimation. To compensate for the reduced intensity levels caused by de-collimation, we used the spare capacity in the lamp controller. Following a simple trigonometric calculation, the lens has been defocused to generate a 25 mm wide light band, an increase that is sufficient to accommodate the slate bowing effects in the range [0, 5 mm] and the vibrations caused by the slate transport system.

The last issue that we confronted during the development of the illumination set-up was the development of software routine that was applied to compensate for the non-linearities in the horizontal profile (longitudinal axis) of the light band. As the fiber optic is 30" long, the profile of the light band shows stronger illumination levels towards the central position when compared to the intensity level supplied at the left and right extremities of the slate. This is illustrated in Figure 7(a) where the unprocessed horizontal light profiles for three reference slates are depicted. To compensate for this uneven response of the illumination unit, we have subtracted the mean intensity level (calculated from all reference slates that are used to train the system) from the unprocessed data and the obtained results are averaged with respect to each pixel position to compute the light compensation map. This light compensation map encodes the deviations from the expected mean intensity level and it is directly used to linearise the unprocessed horizontal profile (see Figure 7b). The application of the horizontal profile linearisation reduced the light variation in the horizontal direction from 20 per cent to 2.5 per cent. The linearisation of the response of the illumination unit in the moving direction was deemed unnecessary, as the light intensity variation in the vertical axis shows negligible variation due to de-collimation.



(a)



(b)

Figure \$.7. Compensation for the non-linearities in the response of the light unit along the horizontal direction. (a) Unprocessed horizontal light profiles. (b) Compensated horizontal light profiles.

\$.6 Slate inspection algorithm

As indicated in Section \$.4 the slate inspection algorithm has been designed in a modular fashion where each component has been optimised to identify one category of visual defects. This approach was appropriate as the modular architecture allows facile system training and more importantly the parameters that need to be optimised for each component can be easily adjusted if changes are made on the specification of the

finite product. To this end, the proposed algorithm involves five distinct computational strands that were tailored to address specific inspection tasks. Full details about each image processing component of the developed inspection algorithm will be provided in the remainder of this section.

\$.6.1 Segmentation of slate from image data and nail hole verification procedure

The first step of the slate inspection algorithm involves the segmentation of the slate from the image data. The identification of the slate boundaries was facilitated by cutting slots in the conveyor base and ensuring that the width of the belt is less than that of the slate. This design choice was implemented to ensure that no light arrives back at the line-scan camera when the slate is not imaged and to provide a sharp rise in the optical signal when the slate arrives at the inspection line. Thus, a simple threshold operation is sufficient to robustly segment the slate data and the segmentation process is followed by the identification of the edges and the four corners of the slate. To avoid computationally expensive procedures required to optimise the image acquisition process, a proximity sensor was employed to activate the line scan sensor prior to the arrival of the slate at the inspection point.

Once the corners of the slate are identified, the next operation verifies if the nail holes are correctly positioned with respect to slate boundaries. The nail hole detection involves a threshold-based segmentation technique since the intensity of the optical signal associated with the nail hole is substantially lower than that given by the slate surface. The developed nail hole checking procedure starts with the identification of the hole that is located on the left hand side of the slate surface. The detected xy coordinates of the nail hole are compared to pre-recorded values and if the procedure passes inspection conditions then the algorithm proceeds with the verification of the remaining two nail holes that are located close to the right-hand side top and bottom slate corners. If the nail checking procedure triggers the absence of a nail hole or an incorrect nail hole placement with respect to slate boundaries, the slate is classed as defective and put aside for rejection or re-work. If the nail holes are correctly positioned, then the algorithm fills them with adjacent slate surface pixel information to prevent the identification of visual faults when the slate data is subjected to the automatic inspection process. Figure \$.8 describes graphically the nail verification procedure.

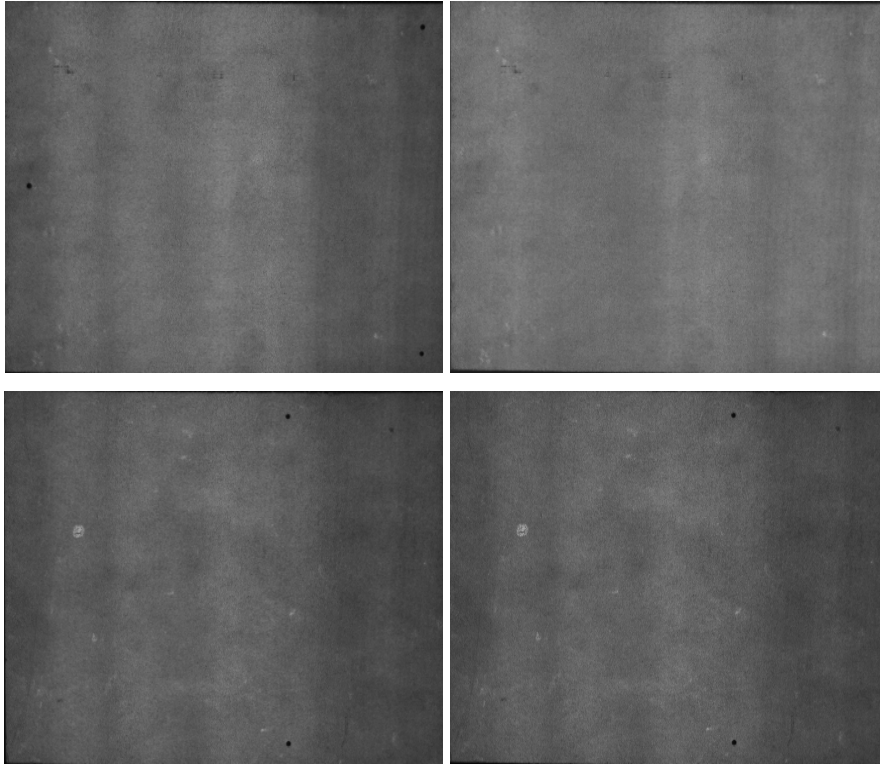


Figure 8.8. Nail hole verification procedure. (Top row) Slate that passes the nail hole verification test. (Bottom row) Slate that fails the nail hole inspection procedure. In the last column the images resulting after the nail hole inspection procedure are displayed. Note that the image that passes the nail hole verification test has the nail hole areas filled with pixels information from adjacent slate surface data to be ready for defect inspection.

6.2 Identification of the visual defects

Prior to the development of the computational modules for visual defect identification, we have analysed the grey level signals associated with reference and defective slates. The experimental trials indicated that the mean grey levels associated with acceptable slates from similar production batches can vary up to 20 grey levels where the overall mean value is 167. To clarify the source of this grayscale variation among reference (non-defective) slates we evaluated the intensity data using different image acquisition approaches. From these experiments we concluded that these variations were not caused by the imperfections in the sensing and optical equipment but rather due to an acceptable variation in the slate surface paint colour. Thus, the image processing procedures that will be

investigated have to sufficiently robust to accommodate this level of inter-slate grayscale variation. In order to identify the computational components of the inspection algorithm we have analysed the gray level signals associated with paint and substrate defects and a summary of the test results is shown in Table 3. This analysis allowed us to analyse the impact of the visual defects on the overall intensity data distribution. Our study revealed that the vast majority of defects have a negligible influence on the overall slate intensity data distribution and this finding clearly indicates that it would be desirable to inspect the slate image in small subsections, as the relative impact of the defect on the grey level statistics is substantially increased. To this end, the slate image was divided into segments of 128×128 pixels and each segment need to be individually processed.

No.	Defect type	Overall slate grayscale mean	Defect grayscale value
1	Lump 1	186	150
2	Lump 2	180	140
3	Lump 3	184	125
4	Lump 4	182	135
5	Lump 5	191	160
6	Insufficient paint	181	136
7	Paint debris	172	80
8	Paint droplet	179	150
9	Spots	184	150
10	Barring	181	166
11	Orange peel	181	127
13	Efflorescence 1	181	135
14	Efflorescence 2	175	150
15	No paint	180	100
16	Shade variation	180	150
17	Template mark 1	177	145
18	Template mark 2	189	140
19	Template mark 3	179	120
20	Template mark 4	180	150
22	Template mark 5	181	150

Table 3. The gray level values associated with a representative sample of visual defects.

Based on the analysis of the grayscale values associated with reference and defective image sections, we have devised an algorithm which consists of four distinct computational strands - in this approach each component has been designed to strongly respond to a narrow category of visual defects. The block diagram of the developed slate inspection algorithm is depicted in Figure \$.9 and the main components can be summarised as follows:

- Global mean threshold method
- Adaptive signal threshold method
- Labeling method
- Edge detection and labeling method.

Each component depicted in Figure \$.9 is applied to each 128×128 segment of the slate image and the results are compared to experimentally determined thresholds. Each component of the slate inspection will be detailed in the remainder of this section.

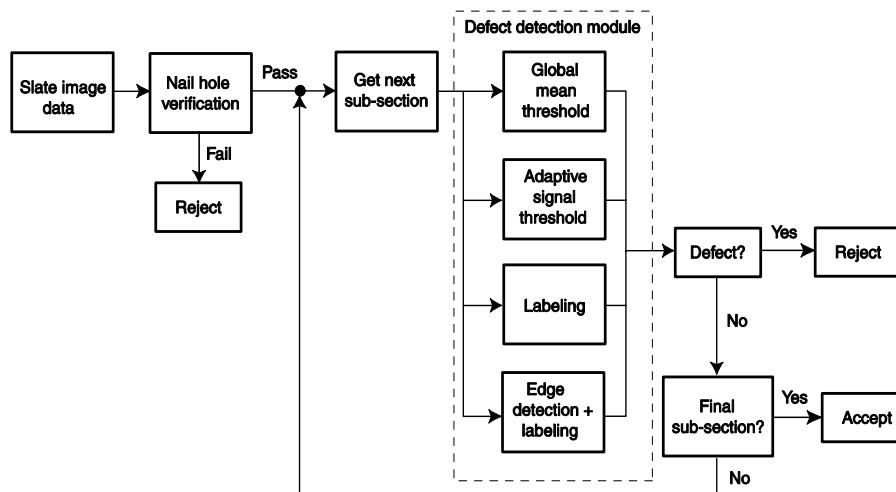


Figure \$.9. Overview of the slate inspection algorithm.

\$.6.3 Global mean threshold method

This component has been developed to evaluate the mean gray level of the image section with the aim of identifying the gross defects that may be present on the surface of the slate. In this regard, the mean value for each subsection is compared to an experimentally determined mean value and this approach proved to be effective in detecting a range of defects including missing paint, orange peel, efflorescence, insufficient paint and severe shade variation.

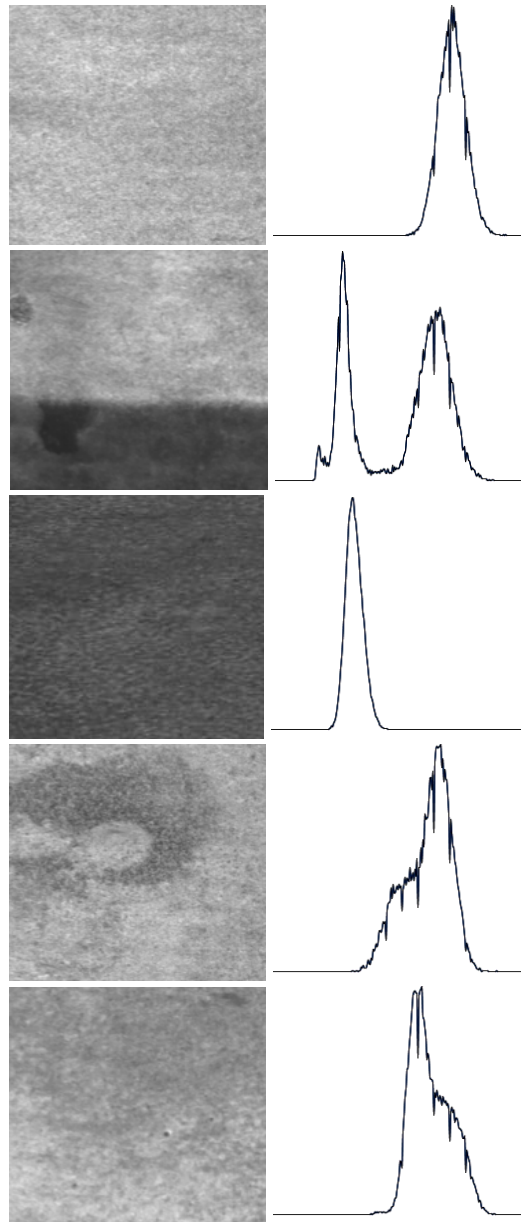


Figure 10. Gross defects identified by the global mean threshold method. (Left) Images showing a reference slate section and slate sections exhibiting gross visual defects. (Right) The corresponding grayscale distributions. From top to bottom, reference (non-defective) slate section, slate section detailing an insufficient paint defect, slate section detailing an orange peel defect, slate section detailing an efflorescence defect and slate section detailing a shade variation defect.

In spite of its simplicity, this method proved to be the most reliable in detecting defects that cover large areas of the slate surface, defects that have a dramatic impact on the grayscale distribution when evaluated at local level (see Figure 10). To increase the robustness of the proposed method a global mean threshold has been employed to identify defects such as missing paint and orange peel and grade specific thresholds were experimentally determined for the identification of low contrast defects such as efflorescence, insufficient paint and shade variation.

6.4 Adaptive signal threshold method

Our experimental measurements indicated that the slate texture induces a grayscale variation for non-defective image sections in the range $[\text{mean} - 30, \text{mean} + 30]$. When analysing the 128×128 image sections for visual defects, to avoid the occurrence of false positives we need to locate the paint and substrate defects outside the range $[\text{mean} - 40, \text{mean} + 60]$. By thresholding the image data with these values a relative large category of visual defects can be robustly identified. The defects detected by this method include missing paint (where less than 50 per cent of the image section is defective), localised paint faults such as paint debris, droplets and spots and structural defects generated by an improper slate formation.

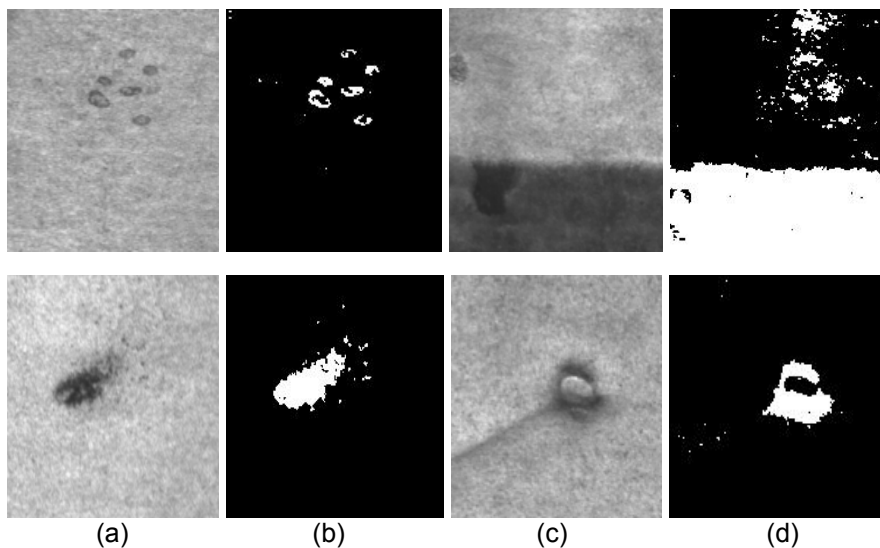


Figure 11. Visual defects identified by the adaptive signal threshold method. (a,c) Defective slate sections. (b,d) Resulting images after the application of the adaptive signal threshold method. Top row - paint defects such as paint droplets and insufficient paint. Bottom row - substrate defects such as burn mark and template mark.

This method has not been found useful in detecting low contrast visual defects such as barring and elongated depressions whose gray levels are within the grayscale variation generated by the slate texture. Representative paint and substrate defects that are detected by the adaptive signal threshold method are depicted in Figure \$.11.

\$.6.5 Labeling method

The aim of this method is to identify the visual defects that cover a relative small area with respect to the overall size of the analysed 128×128 image section. This method consists of several steps that are illustrated in Figure \$.12.

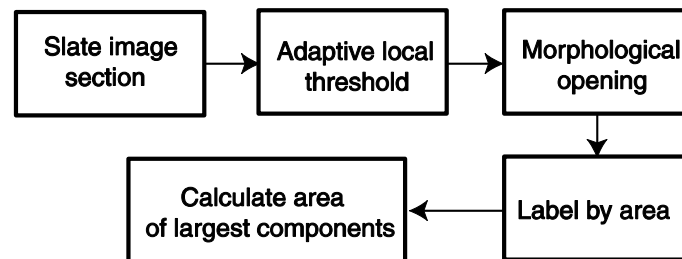


Figure \$.12. Overview of the labeling method.

The first step of the labeling method converts the image corresponding to the analysed slate section into the binary format by applying a local adaptive threshold operation [28]. The aim of this step is to identify the relative bright and dark regions with respect to the local gray mean value. The second step involves the application of a binary opening operation with the aim of removing the small unconnected regions that are caused by the non-regularized slate texture and the image noise. The third step involves the application of the labeling by area operation [28,29] to provide an unique label for each disjoint white blob in the image resulting from the morphological opening step. Since the small blobs are often associated with the slate texture, the largest blobs are of interest as they are generally caused by visual defects. Thus, to reduce the impact of the randomly distributed blobs that are generated by the slate texture, we compute the area of the ten largest blobs and this feature is used to discriminate between reference and defective image sections. This method proved effective in identifying high contrast defects such as droplets, paint debris, spots, efflorescence and template marks. A small collection of visual defects that are identified by the labeling method is depicted in Figure \$.13.

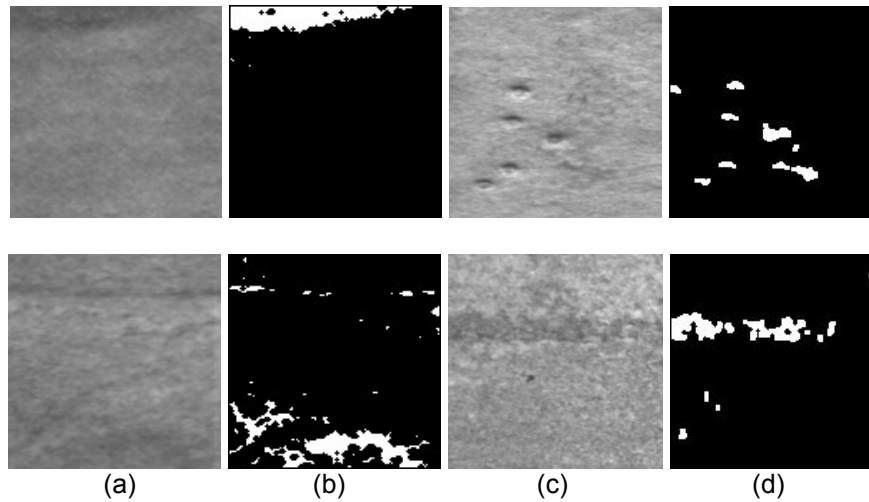


Figure 13. Visual defects identified by the labeling method. (a,c) Defective slate sections. (b,d) Resulting images after the application of the labeling method. Top row - paint defects such as shade variation and paint droplets. Bottom row - substrate defects (template marks).

6.6 Edge detection method

The last component of the inspection algorithm has been designed to specifically detect the narrow elongated defects, as the previously described methods were not sufficiently accurate in identifying this type of slate faults. As this defect identification method is based on the application of first order derivative operators (Sobel edge detector), prior to edge extraction the image data is subjected to median filtering. The experimental measurements carried out during the development phase revealed that narrow defects such as depressions and elongated substrate marks have a shallow intensity profile and as a result gaps are present in the resulting edge structure. To compensate for this issue a morphological closing operator is applied and the resulting data is labeled by area for further analysis. Similar to the approach used for labeling method, the largest ten components were retained and their collective area is used as a discriminative feature to grade the slate section under analysis as acceptable or defective. Figure 14 depicts some representative defects that are identified by the edge detection method.

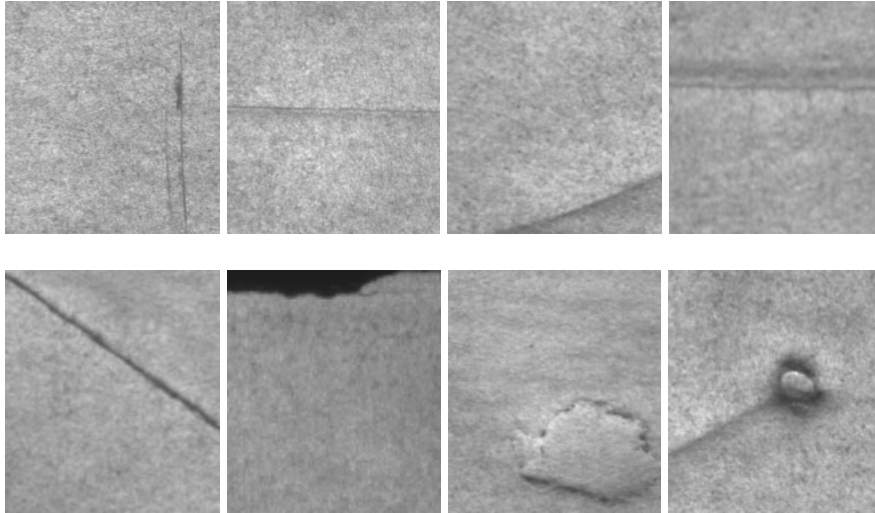


Figure 14. Visual defects identified by the edge detection method. (Top images) Paint defects. (Bottom images) Structural defects.

3.7 Effect of slate bowing on slate inspection

The slate inspection algorithm detailed in Section 3.6 performs the identification of the visual defects on each 128×128 segment of the slate image. To facilitate the tiling of the slate image into sub-sections, the slate was approximated with a rectangle that is obtained by connecting the corners of the slate that have been identified during the slate segmentation process (see Section 3.6.1). This procedure worked very well when applied to flat slates, but generated false triggers when applied to slates that are affected by depth profile variations (slate bowing). These false positives are caused by the displacements between the straight edge obtained by connecting the slate corners and the curved edge of the imaged slate. This slate edge positioning errors lead to an incorrect image tiling and this generates situations when the 128×128 image segments include non-slate image data (background information), while on the opposite side of the slate there are sections of the slate that are not investigated by the inspection algorithm (see the shaded area in Figure 15). This is illustrated in Figure 15 where the problems caused by slate bowing are illustrated. An example that shows the occurrence of false positives due to slate bowing is depicted in Figure 16.

To address this issue, the procedure to identify the slate edges has been modified in order to accommodate the deviations that occur from the straight edge when imaging slates that are affected by depth profile variation. In this regard, the edge that is generated by connecting the slate

corners is divided into shorter lines with 30 mm length and the location of these short segments is identified with respect to the segmented slate data. Using this approach, the image tiling process ensures that the image sub-sections are placed adjacent to these segments and as a result no slate data will be missed by the inspection algorithm or false positives generated by the incorrect positioning of the image sub-segments with respect to the real edge of the slate.

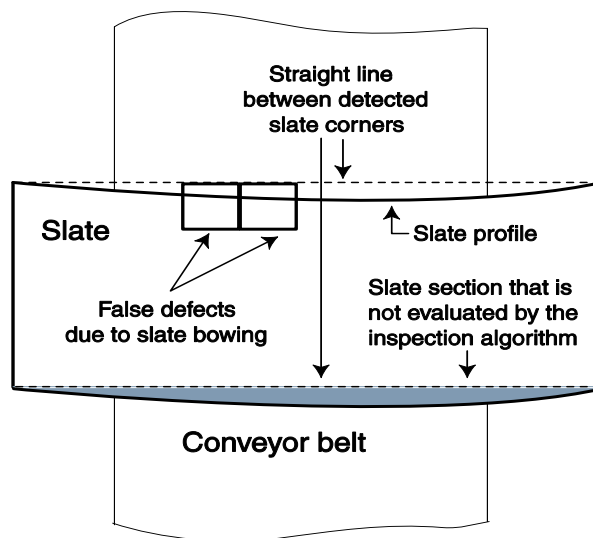


Figure \$.15. False defects generated by slate bowing.

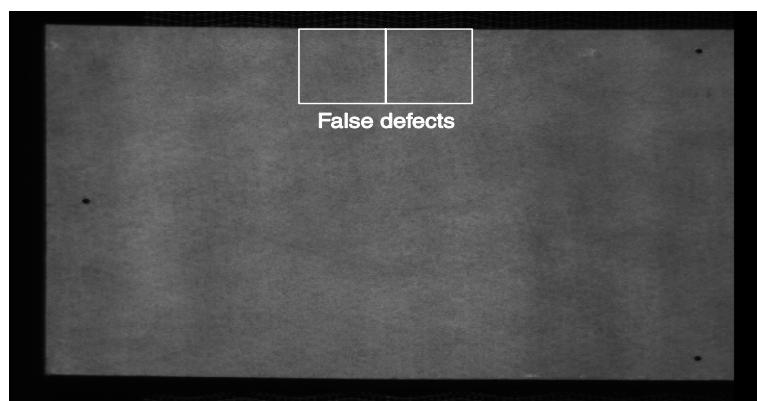


Figure \$16. Example illustrating the false defects caused by slate bowing effects.

\$.8. Experimental results

The conveyor was set at 38 m/min and the camera exposure was set to 400 μ s giving a scan frequency of 2.5 KHz. The variability of the conveyor speed has been measured by imaging a reference slate in succession and the experimental results indicate that the variation profile of the conveyor speed induced a 0.8 per cent variation in the pixel resolution in the moving direction [1]. The variation in the pixel resolution due to inconsistencies in the conveyor speed has negligible effects on the image acquisition process and it was found that it has no negative effects on the inspection results.

Since the inspection algorithm detailed in Section \$.6 entails the optimisation of a large number of threshold parameters, the system has been trained using 400 slates. The developed slate inspection system has been tested on 300 unseen slates that are sampled from different production batches. The 300 slates used in the experimental activity were graded into acceptable and defective units by an experienced operator based on a comprehensive visual examination. The proposed system was able to correctly grade the acceptable slates with an accuracy of 99.32 per cent (148 slates) and the defective slates with an accuracy of 96.91 percent (162 slates). A detailed performance characterisation is provided in Table 4. To qualitatively and quantitatively illustrate the performance attained by the proposed system, in Table 4 the detection rate for each category of defects listed in Table 2 is provided.

Type	Undetected	Detected	Accuracy
Missing paint	0	4	100%
Insufficient paint	0	9	100%
Efflorescence	0	15	100%
Shade variation	0	12	100%
Nozzle drip	0	14	100%
Droplets	0	8	100%
Dust	0	4	100%
Wax	1	7	87.5%
Template marks	2	33	94.28%
Template marks II	0	5	100%
Lumps	0	13	100%
Depressions	1	3	75%
Bad edge	0	18	100%
Misc. types	1	12	92.30%
TOTAL	5	157	96.91%

Table 4. Summary of detection rate for each category of visual defects.

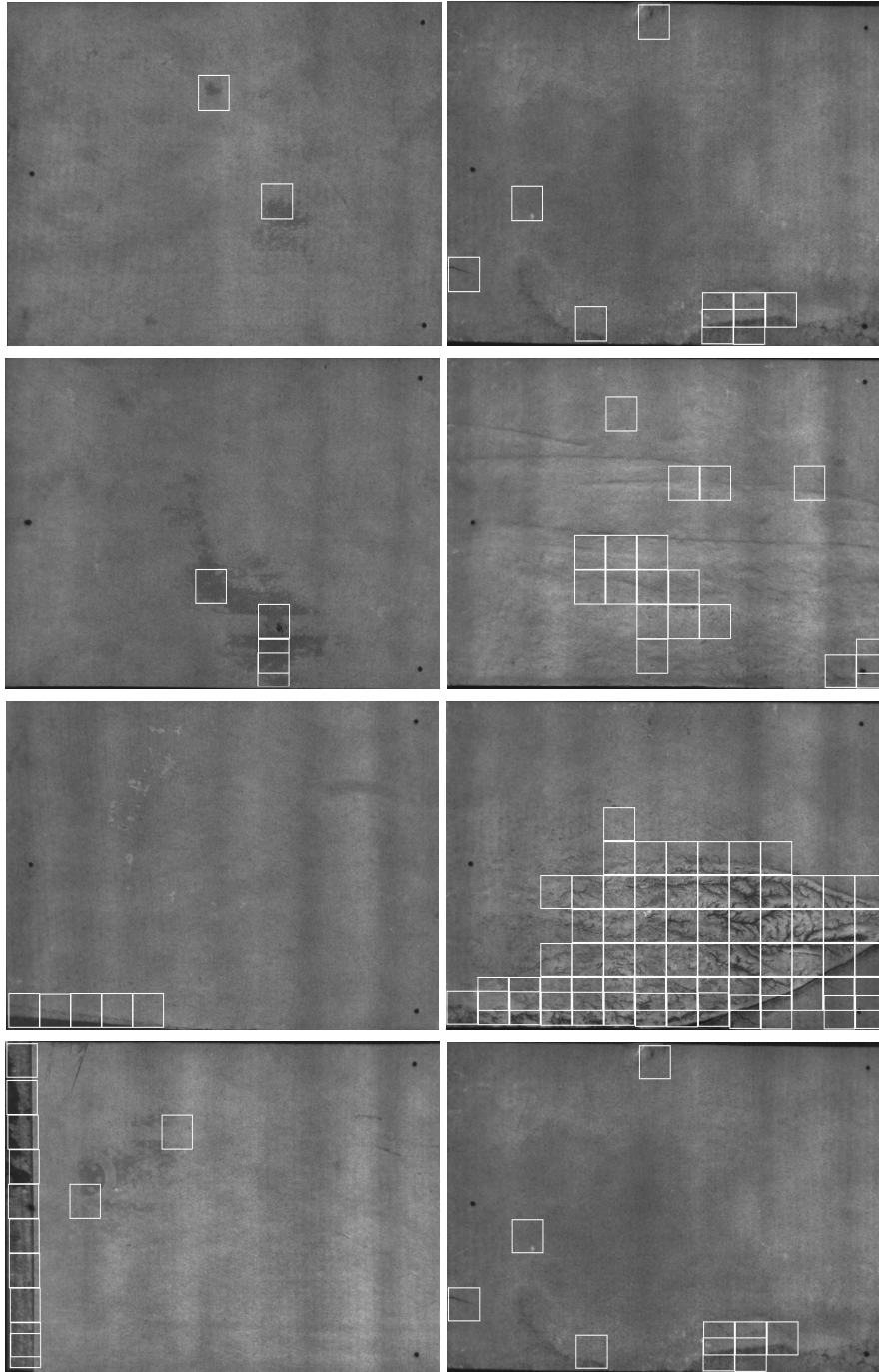


Figure \$.17. Identification of the visual defects on a selection of defective slates that exhibit a large variety of paint and substrate defects.

As indicated in Table 4 the lowest performance of the slate inspection system was achieved in the identification of depressions which is a subclass of substrate defects. The system failed to identify a defective slate containing a shallow depression that was positioned parallel to the moving direction axis. To fully clarify the impact of these defects on the inspection results, we imaged the slate with the short edge facing forward (slate rotated with 90°). Using this slate orientation, the system was able to identify the defect as it produced sufficient contrast when compared to adjacent non-defective areas of the slate. We envision that the detection rate for this type of substrate defect can be substantially increased if the slate is imaged in two orthogonal directions. The inspection system was also not able to identify two small template marks with an area of approx. 1 mm². These defects were missed as their statistical impact on the gray scale distribution of the 128×128 slate segment was very limited and the relaxation of threshold conditions for labeling method was not an option since it will lead to a substantially increase in the number of false positives. Typical inspection results are depicted in Figure \$.17 where white boxes are used to mark the defective image sections. Additional results are illustrated in Figure \$.18 where reference and defective image sections are depicted and the images resulting after the application of the four computational strands of the inspection algorithm are also shown (for the sake of completeness, the pixel count for each method of the inspection algorithm is provided).

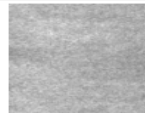

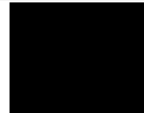






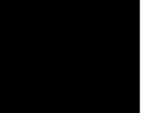
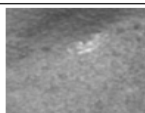




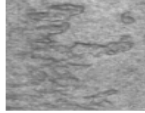

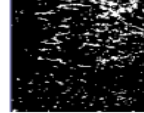


Input image	Adaptive signal component output	Global threshold output	Label component output	Edge component output
 Reference	 11 OK	 OK	 191 OK	 36 OK
 Shade variation	 15 OK	 Defect	 1738 Defect	 2 OK
 Lump	 487 Defect	 Defect	 4020 Defect	 113 Defect
 Template mark	 475 Defect	 Defect	 1442 Defect	 1129 Defect

Figure \$.18. Output of the inspection algorithm for a small set of reference and defective slate sections.

\$.9 Conclusions

The major objective of this chapter was the introduction of a machine vision system that has been developed for the automated inspection of painted slates. Since the development of an industry compliant inspection system requires the identification of optimal solutions for a large spectrum of problems relating to opto-mechanical and software design, in this chapter we provided a comprehensive discussion about each component of the system and we emphasized the difficulties that we had to confront during the development phase of the inspection sensor. The illumination set-up proved in particular challenging as we had to devise a solution that is able to provide sufficient illumination intensity that allows imaging the slate at production line speeds, but at the same time it is able to accommodate non-idealities such as slate depth profile variations and vibrations that are introduced by the slate transport system.

The experimental data indicates that automatic slate inspection can be achieved and the installation of the proposed inspection system in a manufacturing environment is a realistic target. The evaluation of the inspection prototype in a factory-style manner was an important part of the development process, as it allowed us to sample, address and optimize a large number of hardware and software design choices that are required for robust slate inspection. The proposed inspection system attained 96.91 per cent overall accuracy in detecting the visual defect present on the slate surface and this level of performance indicates that the devised machine vision solution can be considered as a viable option in replacing the existing manual inspection procedure.

Acknowledgements: We would like to acknowledge the valuable contribution of our industrial partner during the development phase of our slate inspection system and Enterprise Ireland for its generous financial support.

References

1. Ghita O, Whelan PF and Carew T, A vision-based system for inspecting painted slates, *Sensor Review*, 26(2), 2006: 108-115.
2. Ghita O, Whelan PF, Carew T and Nammalwar P, Quality grading of painted slates using texture analysis, *Computers in Industry (Special Issue on Machine Vision)*; 56(8-9), 2005: 802-815.
3. Tobias O, Seara R, Soares F and Bermudez J, Automated visual inspection using the co-occurrence approach, *Proc. of the IEEE Midwest Symposium on Circuits and Systems*, pp. 154-157, 1995.
4. Porter AL, Rossini FA, Eshelman BJ, Jenkins DD and Cancelleri DJ, Industrial robots, a strategic forecast using the technological delivery system approach, *IEEE Transactions on Systems, Man and Cybernetics*, 15(4), 1985: 521-527.

5. Batchelor BG and Waltz FM (2001), *Intelligent Machine Vision: Techniques, Implementations and applications*, Springer, New York, USA, ISBN 978-3540762249.
6. Ghita O, Whelan PF, A bin picking system based on depth from defocus, *Machine Vision and Applications*, 13(4), 2003: 234-244.
7. Batchelor BG and Whelan PF (1997), *Intelligent Vision Systems for Industry*, Springer, ISBN 978-3540199694.
8. Peñaranda J, Briones L and Florez J, Colour machine vision system for process control in ceramics industry, *Proc. of SPIE*, vol. 3101, pp. 182-192, 1997.
9. Boukouvalas C, De Natale F, De Toni G, Kittler J, Marik R, Mirmehdi M, Petrou M, Le Roy P, Salgari R and Vernazza F, An integrated system for quality inspection of tiles, *Proc. of the International Conference on Quality Control by Artificial Vision*, pp. 49-54. 1997.
10. Boukouvalas C, Kittler J, Marik R and Petrou M, Automatic color grading of ceramic tiles using machine vision, *IEEE Transactions on Industrial Electronics*, 44(1), 1997: 132-135.
11. Boukouvalas C, Kittler J, Marik R and Petrou M, Colour grading of randomly textured ceramic tiles using colour histograms, *IEEE Transactions on Industrial Electronics*, 46(1), 1999: 219-226.
12. Carew T, Ghita O and Whelan PF, Exploring the effects of a factory-type test-bed on a painted slate detection system, *International Conference on Mechatronics*, pp. 365-370, 2003.
13. Fernandez C, Fernandez J and Aracil R, Integral on-line machine vision inspection in the manufacturing process of ceramic tiles, *Proc. of the SPIE*, vol. 3306, 1998.
14. Müller S and Nickolay B, Morphological image processing for the recognition of surface defects, *Proc. of SPIE*, vol. 2249, pp. 298-307, 1994.
15. Sternberg SR, A morphological approach to finished surface inspection, *Proc. of the IEEE International Conference on Acoustics, Speech, Signal Processing*, pp. 462-465, 1985.
16. Kuleschow A, Münzenmayer M, Spinnler K, A fast logical-morphological method to segment scratch - type objects, *Proc. of the International Conference on Computer Vision and Graphics*, pp. 14-23, 2008.
17. Costa CE and Petrou M, Automatic registration of ceramic tiles for the purpose of fault detection, *Machine Vision and Applications*, 11(5), 2000: 225-230.
18. Mäenpää T, Viertola J and Pietikäinen M, Optimising colour and texture features for real-time visual inspection, *Pattern Analysis and Applications*, 6(3), 2003: 169-175.
19. Kyllönen J and Pietikäinen M, Visual inspection of parquet slabs by combining color and texture, *Proc. of the IAPR Workshop on Machine Vision Applications*, pp. 187-192, 2000.

20. Latif-Amet A, Ertüzün A, and Erçil A, Efficient method for texture defect detection: sub-band domain co-occurrence matrices, *Image and Vision Computing*, 18(6-7), 2000: 543-553.
21. X. Xie, A review of recent advances in surface defect detection using texture analysis techniques, *Electronic Letters on Computer Vision and Image Analysis*, 7(3), 2008: 1-22.
22. Mandriota C, Nitti M, Ancona N, Stella E and Distanto A, Filter-based feature selection for rail defect detection, *Machine Vision and Applications*, 15(4), 2004: 179-185.
23. Kukkonen S, Kälviäinen H and Parkkinen J, Color features for quality control in ceramic tile industry, *Optical Engineering*, 40(2), 2001: 170-177.
24. Smith ML and Stamp RJ, Automated inspection of textured ceramic tiles, *Computers in Industry*, 43(1), 2000: 73-82.
25. Picon A, Ghita O, Whelan PF and Iriondo PM, Fuzzy spectral and spatial feature integration for classification of non-ferrous materials in hyper-spectral data, *IEEE Transactions on Industrial Informatics*, 5(4), 2009: 483-494.
26. Ojala T, Pietikäinen M and Mäenpää T, Multiresolution gray-scale and rotation invariant texture classification with local binary patterns, *IEEE Transactions on Pattern Analysis and Machine Intelligence*, 24(7), 2002: 971-987.
27. Newman T and Jain A, A survey of automated visual inspection, *Computer Vision and Image Understanding*, 61(2), 1995: 231-262.
28. Whelan PF and Molloy D (2000), *Machine Vision Algorithms in Java, Techniques and Implementation*, Springer (London), ISBN: 1-85233-218-2.
29. Davies ER (1997), *Machine Vision: Theory, Algorithms, Practicalities*, 2nd edition Academic Press, ISBN: 0-12-206092-X.